Original Article

The efficacy of plasma exosomal miRNAs as predictive biomarkers for PD-1 blockade plus chemotherapy in gastric cancer

Yunqi Hua[1], Shuang Luo[2], Qian Li[3], Ge Song[2], Xiaoling Tian[2], Peng Wang[4], Hongwei Zhu[4], Shuang Lv[5], Xinyi Zhang[5], Zixuan Yang[2], Geoffrey Ku[6], Guo Shao[1]

[1]Department of Public Health, International College, Krirk University, Bangkok, Thailand; [2]Baotou Medical College, Inner Mongolia University of Science and Technology, Baotou, China; [3]Lianchuan Biotechnology Co., Ltd., Hangzhou, China; [4]The Second Affiliated Hospital of Baotou Medical College, Baotou, China; [5]Department of Pharmacy, Baotou Cancer Hospital, Baotou, China; [6]Gastrointestinal Oncology Service, Department of Medicine, Memorial Sloan Kettering Cancer Center, New York, NY, USA

Contributions: (I) Conception and design: Y Hua, G Shao; (II) Administrative support: Y Hua; (III) Provision of study materials or patients: Q Li, S Luo, S Lv, X Zhang; (IV) Collection and assembly of data: S Luo, G Song, X Tian, P Wang, H Zhu, S Lv, X Zhang, Z Yang; (V) Data analysis and interpretation: S Luo, G Song, X Tian, P Wang, H Zhu, S Lv, X Zhang, Z Yang; (VI) Manuscript writing: All authors; (VII) Final approval of manuscript: All authors.

Correspondence to: Guo Shao, PhD. Department of Public Health, International College, Krirk University, No. 3 soi Ramintra 1, Ramintra Road, Anusaowaree, Bangkhen, Bangkok 10220, Thailand. Email: shao.guo.china@gmail.com.

Background: The response of gastric cancer (GC) patients to first-line programmed cell death 1 (PD-1) blockade and S-1 plus oxaliplatin (SOX) chemotherapy varies considerably, and the underlying mechanisms driving this variability remain elusive. Exosomal microRNAs (miRNAs or miRs) have emerged as potential biomarkers for efficacy prediction due to their roles in GC biology and stable expression in serum. In this study, we aimed to identify biomarkers to predict patients' response to anti-PD-1 therapy and further elucidate the potential mechanisms by which these exosomal miRNAs modulate the immune response in GC.

Methods: Serum exosomes were extracted from 11 GC patients (five in the primary cohort and six in the validation cohort) treated with SOX and camrelizumab (a PD-1 inhibitor). High-throughput sequencing was performed to identify miRNA expression profiles, after which hierarchical clustering and a differential expression analysis were conducted. Functional enrichment analyses of the target genes for the significantly upregulated miRNAs were performed using the Gene Ontology (GO) and Kyoto Encyclopedia of Genes and Genomes (KEGG) databases. The validation of the candidate miRNAs was carried out by quantitative polymerase chain reaction (qPCR) in an independent cohort.

Results: MiRNA sequencing identified 3,083 miRNAs, of which 74 (42 upregulated and 32 downregulated) were differentially expressed between the responders and non-responders. The GO and KEGG pathway analyses of the top 20 upregulated miRNAs indicated that the target genes were significantly involved in transcription regulation, cytoplasmic processes, and protein binding, and that key pathways included the PI3K-AKT, MAPK, RAP1, and RAS signaling pathways. Consistent with the sequencing findings, the qPCR validation results showed significant differences in the expression levels of miRNA451a and miRNA142-5p between the responders and non-responders.

Conclusions: This study identified specific plasma exosomal miRNAs in GC patients that differ between responders and non-responders to PD-1 monoclonal antibody therapy combined with chemotherapy. These miRNAs could serve as predictive biomarkers, paving the way for precision medicine and personalized therapy in the treatment of GC.

Keywords: Gastric cancer (GC); plasma exosomal microRNA (plasma exosomal miRNA); immunotherapy plus chemotherapy; efficacy prediction

Submitted Nov 01, 2024. Accepted for publication Nov 18, 2024. Published online Nov 27, 2024.
doi: 10.21037/tcr-24-2151
View this article at: https://dx.doi.org/10.21037/tcr-24-2151

Introduction

With the fifth highest incidence and mortality rates, gastric cancer (GC) is among the most prevalent gastrointestinal malignancies worldwide (1). Despite advances in treatment modalities, challenges persist in effectively predicting therapeutic the response, particularly in the context of programmed cell death 1 (PD-1) monoclonal antibody therapy. Early stage GC often presents asymptomatically, leading to delayed diagnoses and missed opportunities for optimal surgical intervention (2). Thus, there is an urgent need to identify more effective predictive markers to guide treatment decisions and improve patient outcomes.

PD-1 monoclonal antibodies, which target the PD-1 receptor on T cells, have emerged as promising agents in GC therapy. Clinical investigations have shown the efficacy of these antibodies in combination with chemotherapy in treating GC, which have been shown to result in improvements in objective response rates and prolonged progression-free survival and overall survival (3-5). In current clinical practice, PD-1 inhibitors combined with S-1 plus oxaliplatin (SOX) chemotherapy has become a standard first-line treatment option for patients with advanced gastric cancer, particularly for those without other actionable targets such as Human epidermal growth factor receptor 2 (HER-2) or high programmed cell death ligand 1 (PD-L1) expression. In cases lacking targetable mutations or biomarkers, the use of PD-1 inhibitors in combination with chemotherapy is preferred as the initial therapeutic approach. While PD-L1 positive cancers are more likely to respond to immunotherapy plus chemotherapy combinations, most patients with PD-L1 positive cancers derive only modest benefit. As such, there remains an urgent need to identify the factors influencing PD-1 monoclonal antibody efficacy and elucidate the underlying mechanisms that govern their therapeutic effectiveness.

Exosomal microRNAs (miRNAs or miRs) have garnered increasing attention in GC biology, as they appear to play pivotal roles in proliferation, metastasis, and drug resistance. These miRNAs facilitate intercellular communication and modulate key cellular processes, such as autophagy, apoptosis, and inflammation, making them promising candidates for predicting the treatment response (6,7). Extensive mechanism research has shown the significant role of exosome-derived RNAs in cancer cell proliferation and invasion (8). Previous studies have suggested the potential utility of exosomal miRNAs in predicting the therapeutic response among GC patients undergoing PD-1 monoclonal antibody treatment (9,10). Given their stable expression and the ease with which they can be detected, serum exosome miRNAs hold promise as biomarkers for predicting the treatment response, and could also pave the way for precision medicine and personalized therapy. Recently, a necroptosis-associated miRNA signature was identified that effectively predicts patient prognosis and the immune landscape in stomach adenocarcinoma, enhancing our understanding of the pathogenesis of GC and offering potential clinical applications for personalized immunotherapy (11).

In this study, we used bioinformatics methodologies to analyze high-throughput sequencing data of plasma exosomal miRNAs from patients undergoing PD-1 monoclonal antibody therapy combined with chemotherapy. Our objective was to delineate specific miRNA expression profiles for responders and non-responders and elucidate their mechanistic effects on treatment outcomes. By identifying plasma exosomal miRNAs predictive of the treatment response, we sought to contribute to the development of precision medicine approaches in GC therapy. We present this article in accordance with the MDAR reporting checklist (available at https://tcr.amegroups.com/article/view/10.21037/tcr-24-2151/rc).

Highlight box

Key findings

- This study identified specific plasma exosomal microRNAs (miRNAs or miRs) that differ between responders and non-responders to programmed cell death 1 (PD-1) blockade combined with chemotherapy in gastric cancer (GC) patients. The miRNAs miR-451a and miR-142-5p were confirmed to be significantly associated with the treatment response.

What is known, and what is new?

- Exosomal miRNAs are stable in circulation and implicated in various aspects of cancer biology, including GC. Previous research has established a role for miRNAs in cancer progression and response to treatment.
- This study identifies miR-451a and miR-142-5p as predictive biomarkers for the efficacy of immunotherapy in gastric cancer. Importantly, these miRNAs may offer a non-invasive method for predicting treatment outcomes, potentially enabling personalized treatment strategies.

What is the implication, and what should change now?

- Our findings suggest the exosomal miRNA profiles could be used to establish personalized treatment strategies for GC patients. Future clinical approaches should incorporate miRNA testing to better stratify the patients likely to benefit from PD-1 blockade therapy, thus optimizing therapeutic decision making and improving patient outcomes.

Methods

Patient and sampling details

The study was conducted in accordance with the Declaration of Helsinki (as revised in 2013). The study was approved by the Ethics Committee of the Baotou Cancer Hospital (No. 2023001) and informed consent was taken from all the patients. Blood samples were collected from five advanced GC patients at Baotou Cancer Hospital, Inner Mongolia from June 2018 to June 2023 for next-generation sequencing. To be eligible for inclusion in this study, the patients had to meet the following inclusion criteria: (I) be aged ≥18 years; (II) have an Eastern Cooperative Oncology Group performance status score ≤2; (III) have histologically and/or cytologically confirmed gastric adenocarcinoma; and (IV) have undergone treatment for *de novo* advanced GC, including unresectable locally advanced (stage III) or metastatic (stage IV) GC. All the patients in this study, including six other patients who underwent quantitative polymerase chain reaction (qPCR) validation, received a first-line treatment regimen of camrelizumab (200 mg intravenously on day 1 every 3 weeks) combined with SOX (oxaliplatin, 130 mg/m^2 intravenously on day 1 every 3 weeks; S-1, 40 mg/m^2 orally twice daily for 14 days followed by 7 days off), and without any concurrent treatments administered. To analyze the dynamic changes induced by the therapeutic intervention, plasma samples were prepared post-treatment. Treatment response was evaluated after completing two cycles of treatment (each cycle lasting 21 days). According to the Response Evaluation Criteria in Solid Tumors (RECIST 1.1), the patients who achieved a partial response or complete response, defined as the best response observed following treatment were categorized as the responder (R) group (N=3), while the patients with progressive disease or stable disease were included as the non-responder (NR) group (N=2).

Exosome isolation

The plasma samples were centrifuged at 1,000 rmp for 5 min. The exosomes were precipitated from the supernatant using Minute™ high-efficiency exosome precipitation reagent EI-027 (Invent Biotechnologies, CA, USA) in accordance with the manufacturer's instructions.

Exosome characterization

The purified exosomes underwent verification by electron microscopy. Specifically, 5 µL of purified samples was dropped on copper-coated grids. After staining with 2% uranyl acetate for 1 min, any excessive dye was removed, and the grids were dried at room temperature for several minutes. The samples were then visualized at 100 kv on a transmission electron microscope (TEM).

MiRNA sequencing and data analysis

Trizol reagent (Thermo Fisher Technology Co., Ltd., CA, USA) was used to extract the total RNA from samples in accordance with the manufacturer's protocol. The purity and fragment integrity of the extracted total RNA from the samples were determined using NanoDrop ND-1000 (Wilmington, DE, USA) and the 2100 Bioanalyzer (Agilent Technologies, Santa Clara, CA, USA). Total RNA was subjected to miRNA sequencing via single-end sequencing on the Illumina Hiseq 2500 platform (Hangzhou Lianchun Biotechnology Co., Ltd., Hangzhou, China). Briefly, the ligation of 3' and 5' adapters to the total RNA was followed by the reverse transcription and amplification of the RNA using polymerase chain reaction (PCR), which resulted in the enrichment and barcoding of the complementary DNA (cDNA). The PCR products from the library preparation underwent gel electrophoresis before sequencing.

Raw miRNA sequencing reads were processed using ACGT101-miR (version 4.2) to remove unwanted sequences and mapped to miRBase 22.1 to identify known and novel miRNAs. Subsequently, basic local alignment search tool (BLAST) searches and an RNA-fold analysis were conducted for further characterization and genomic localization. A differential expression analysis was performed using the Student's *t*-test, and a $|\log_2 (\text{fold change})| \geq 1$ and a P value <0.05 were considered significant. The targets of exosomal miRNAs were identified by two online databases: Targetscan (http://www.targetscan.org/) and miRanda (http://www.microrna.gr). A Gene Ontology (GO) analysis and Kyoto Encyclopedia of Genes and Genomes (KEGG) pathway analysis were performed using the OmicStudio (https://www.omicstudio.cn/tool) with an adjusted P value <0.05.

Validation of MiRNA by qPCR

Based on the results of the high-throughput sequencing, miR-451a and miR-142-5p were chosen as the indicators for further verification in the six other GC patients (N=3 in both the R and NR groups). The total RNAs in the exosomes were collected by applying Trizol reagent. The cDNA was then synthesized using the Mir-X miRNA First-

Table 1 Demographic and clinical characteristics of discovery cohort patients (n=5)

Characteristics	Responder (n=3)	Non-responder (n=2)
Age, median [range]	74 [70–75]	74 [73–75]
Gender, n (%)		
Female	1 (33.33)	1 (50.00)
Male	2 (66.67)	1 (50.00)
PD-L1 (CPS), n (%)		
>10	1 (33.33)	1 (50.00)
1–10	2 (66.67)	0
<1	0	1 (50.00)
Tumor location, n (%)		
Esophagogastric junction & Fundus of stomach	1 (33.33)	1 (50.00)
Body of stomach	1 (33.33)	0
Antrum	1 (33.33)	0
Lesser curvature of stomach	0	1 (50.00)
MMR/MSI, n (%)		
MSS	3 (100.00)	2 (100.00)
Histology, n (%)		
Signet-ring cell	0	1 (50.00)
Poorly differentiated adenocarcinoma	2 (66.67)	0
Moderately differentiated adenocarcinoma	1 (33.33)	1 (50.00)

PD-L1, programmed death-ligand 1; CPS, combined positive score; MMR, mismatch repair; MSI, microsatellite instability; MSS, microsatellite stability.

Strand Synthesis Kit (Baori Medical Technology, Beijing, China). The following primer sequences were used: miR-451a: 5'AAA CCG TTA CCA TTA CTG AGT T 3'; and miR-142-5p: 5'CAT AAA GTA GAA AGC ACT ACT 3'. U6 small nuclear RNA was used as the internal control. The relative levels of the miRNAs were normalized to U6 and calculated as $2^{-\Delta Ct}$, where ΔCt was calculated as follows: ΔCt = (Ct value of candidate miRNA) – (Ct value of U6).

Western blot

Total exosomal protein was extracted by radioimmunoprecipitation assay buffer (Biyuntian Biotechnology Co., Ltd., Shanghai, China). Sodium dodecyl-sulfate polyacrylamide gel electrophoresis was used for the electrophoresis. The protein was transferred to polyvinylidene difluoride (PVDF) membranes. The PVDF membranes were then blocked and incubated with primary antibodies at 4 ℃ overnight. The following primary antibodies were used: CD63 (1:1,000, sc-5275), HSP70 (1:1,000, sc-32239), and TSG101 (1:1,000, sc-7964). After incubating with secondary antibodies for 1 h at room temperature, the PVDF membranes were then added to Enhanced Chemiluminescence substrate to visualize the protein bands on the gel imaging system Tanon 4600 (Biotanon, Shanghai, China).

Statistical analysis

SPSS software (version 20.0; SPSS, Inc., Chicago, IL, USA) was used for the data analysis. The data were presented as the mean ± standard deviation for the miRNAs. Values were obtained from three independent experiments, using three biological replicates per condition. The Student's *t*-test was used for the further two-group analysis of all the normally distributed measurement data. A P value <0.05 was considered statistically significant.

Results

Identification and characterization of plasma exosomes

The plasma exosomes were isolated from samples obtained from five advanced GC patients (*Table 1*). Among these patients, three presented with locally advanced disease (stage III), characterized by abdominal lymph node metastasis and tumor invasion into surrounding tissues, while two had stage IV disease with distant metastases (one with thoracic metastasis and one with liver metastasis). Of these five patients, three were male and two were female, with a median age of 74 years (range, 70–75 years). These patients were treated with camrelizumab and the SOX regimen. To assess the quality and purity of the extracted exosomes, these particles were first visualized by TEM, which revealed membrane-bound spherical structures of approximately 40–150 nm in both the R and NR groups (*Figure 1A*,*1B*), consistent with the typical characteristics of exosomes. The Western blot analysis confirmed that the known exosomal markers (CD63, HSP70, and TSG101) were highly expressed in our extracted particles (*Figure 1C*). Thus, the populations of the exosomes were highly purified, as indicated by the clear detection of the exosomal markers,

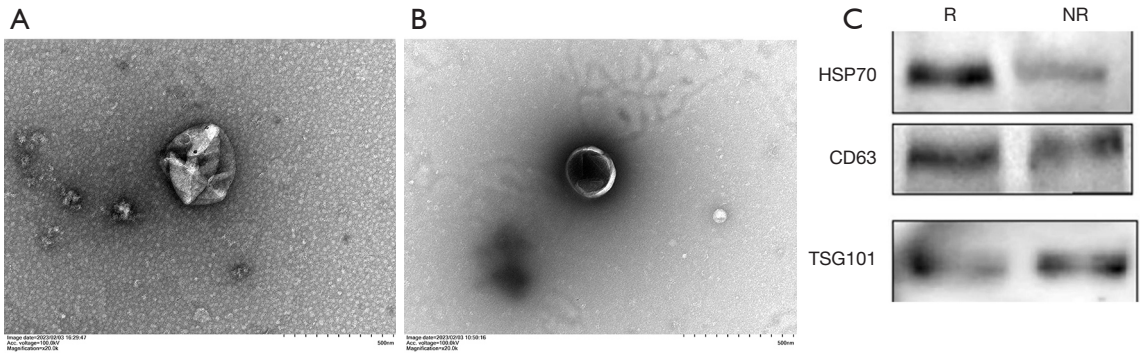

Figure 1 Characterization of exosomes based on morphology and antigen expression. (A,B) Exosome morphological detection in the responder (A) and non-responder (B) group by TEM. Scale bar: 500 nm. (C) Detection of exosomal markers by Western blot (R, responder group; NR, non-responder group). TEM, transmission electron microscope.

and the characteristic morphology observed by TEM.

Exosomal MiRNA expression profiles

High-throughput sequencing was performed to comprehensively screen the candidate miRNAs. The exosomal miRNA differential expression analysis included samples from three patients in the R group and two patients in the NR group, providing a preliminary comparative analysis between the treatment responses. In total, 3,083 miRNAs were identified in the pooled plasma exosome samples of both groups. Hierarchical clustering enabled differentiation between the R and NR groups based on the miRNA expression profiles as shown in a heat map (*Figure 2A* and https://cdn.amegroups.cn/static/public/tcr-24-2151-1-1.xlsx). Using a threshold of a fold change ≥2 and a P value <0.05, 74 differentially expressed miRNAs were identified as significantly altered, of which 42 were upregulated and 32 were downregulated (*Figure 2B*, https://cdn.amegroups.cn/static/public/tcr-24-2151-1-2.xlsx). The results of a further correlation analysis of the differentially expressed miRNAs between the R and NR groups are presented in *Figure 2C*. The top 20 miRNAs with the highest $|\log_2$ (fold change)$|$ values in each group were also identified (*Figure 2D* and https://cdn.amegroups.cn/static/public/tcr-24-2151-1-3.xlsx).

Functional enrichment analysis

To examine the potential mechanisms underlying the isolated miRNAs, target gene prediction was conducted of the top 20 significantly upregulated miRNAs. Subsequently, an enrichment analysis of the identified target genes was carried out using the GO (http://www.geneontology.org) and KEGG (http://www.genome.jp/kegg/) databases.

In the GO analysis, the target microRNAs were divided into the following three categories: biological processes (BPs), cellular components (CCs), and molecular functions (MFs). In this study, a Q value of <0.001 indicated significant enrichment, and a higher rich factor indicated a greater degree of enrichment. As *Figure 3A-3C* show, the regulation of transcription by RNA polymerase II (GO:0006357, rich factor: 0.81), cytoplasm (GO:0005737, rich factor: 0.81), and protein binding (GO:0005515, rich factor: 0.77) were the most highly enriched terms of the BPs, CCs, and MFs, respectively (https://cdn.amegroups.cn/static/public/tcr-24-2151-1-4.xlsx), which suggests that these target genes mostly played a significant role in cytoplasmic process, transcription, etc. (*Figure 3D*).

In the KEGG pathway analysis, a large proportion of the target genes were enriched in various pathways, such as signal transduction and metabolism (*Figure 3E*). Additionally, pathways such as the PI3K-AKT, MAPK, RAP1, and RAS signaling pathways may provide critical insights into the mechanisms underlying the patient response to PD-1 monoclonal antibody therapy combined with chemotherapy (https://cdn.amegroups.cn/static/public/tcr-24-2151-1-5.xlsx).

Validation of the candidate MiRNAs by qPCR

Based on the high-throughput sequencing results, miRNA451a and miRNA142-5p were selected from the upregulated miRNAs for further validation by qPCR. The

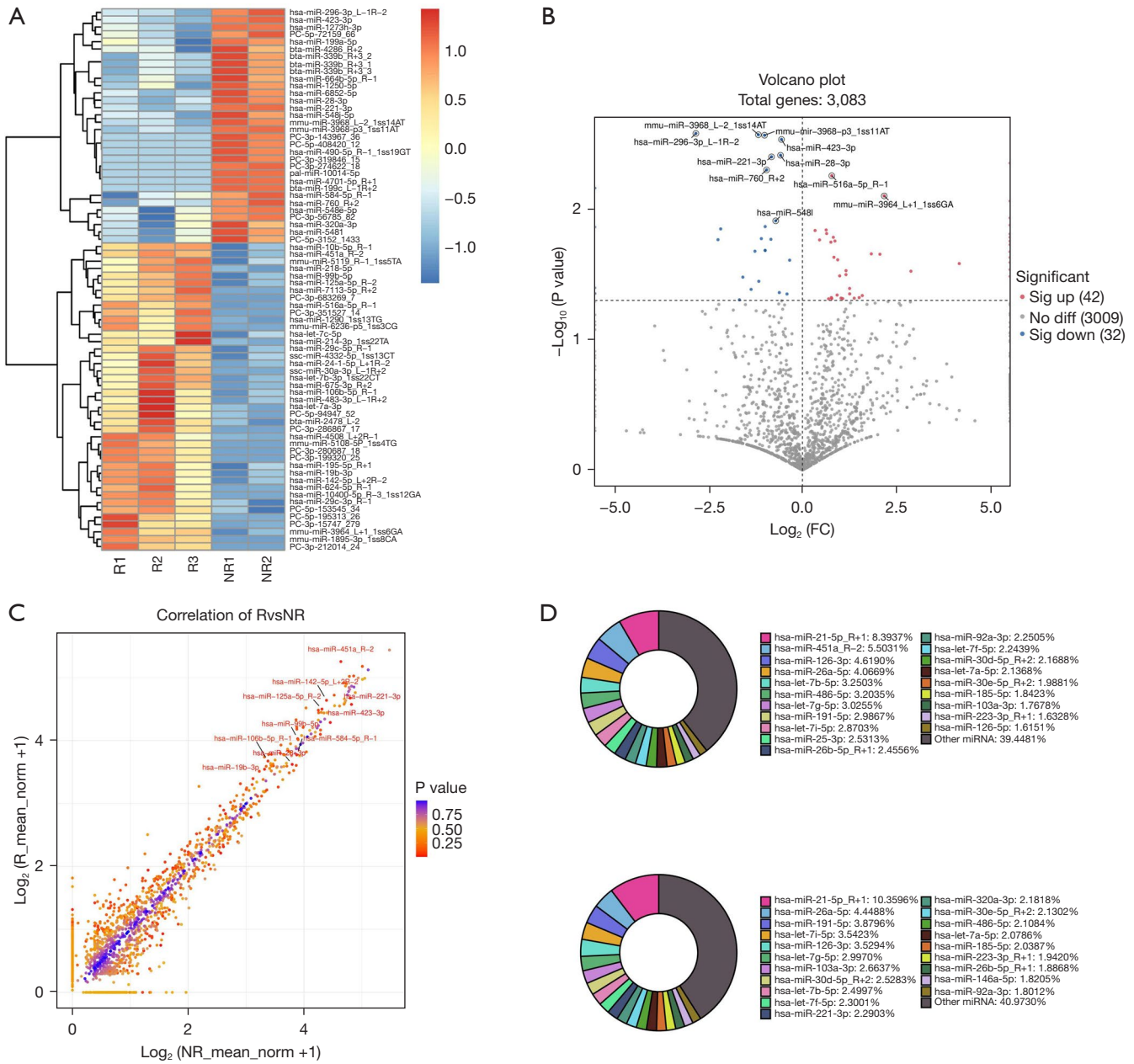

Figure 2 Differential expression analyses and gene expression signature for the responder (R) and non-responder (NR) groups. (A) The panel of exosomal miRNAs to identify potential responders to treatment in advanced GC patients. (B) Volcano plot depicting differential miRNA expression between the R and NR groups. Each point represents a miRNA, with red points indicating significantly upregulated miRNAs (n=42), blue points indicating significantly downregulated miRNAs (n=32), and gray points indicating non-significant changes. The x-axis represents the $\log_2$ fold change in miRNA expression between the R and NR groups, while the y-axis represents the $-\log_{10}$ adjusted P value. (C) Correlation plot showing the expression levels of miRNAs in the two groups. (D) Top 20 miRNAs in the R group (upper panel) and NR group (lower panel). FC, fold change; miRNA, microRNA; GC, gastric cancer.

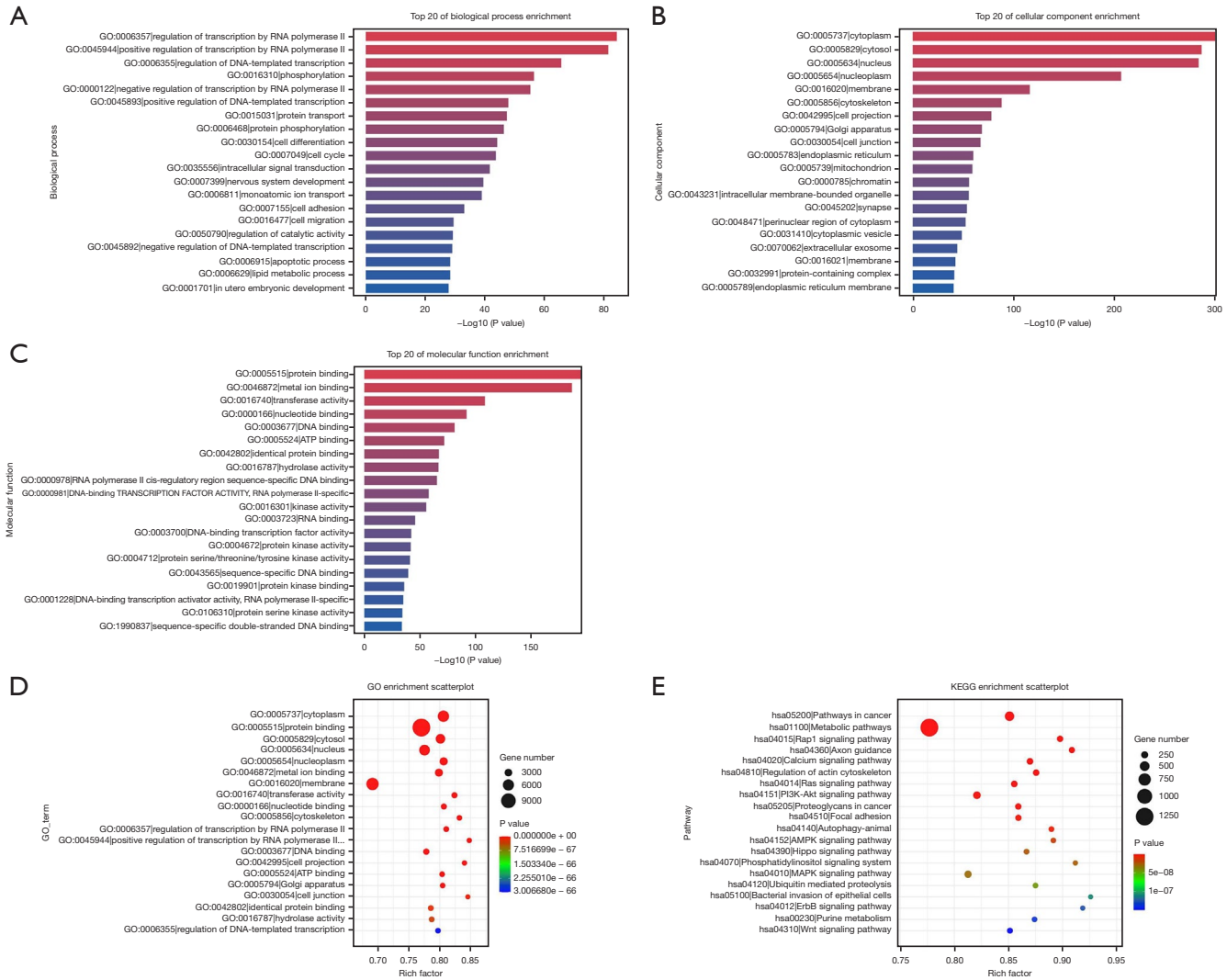

Figure 3 GO enrichment and KEGG pathway analyses of the differentially expressed top 20 miRNAs between the two groups. (A-C) The bar plot illustrates the enriched GO terms for the BP (A), CC (B), and MF categories (C). The x-axis represents $-\log_{10}$ (P value), while the y-axis represents individual GO terms. (D,E) Bubble plot illustrating the enriched GO terms (D) or KEGG pathways (E); the size of the bubbles represents the number of genes involved, and the color represents the significance level. GO, Gene Ontology; KEGG, Kyoto Encyclopedia of Genes and Genomes; BP, biological process; CC, cellular component; MF, molecular function.

independent validation cohort comprised six GC patients treated with camrelizumab and chemotherapy, including three responders (R group) and three non-responders (NR group) (*Table 2*). In this cohort, four patients had locally advanced disease (stage III) with abdominal lymph node metastasis and invasion into surrounding tissues, while two patients had stage IV disease with distant metastases (one with liver metastasis and one with lung metastasis). The results revealed a significant difference in the expression levels of both candidate miRNAs between the two groups (*Figure 4A,4B*, P<0.05). These qPCR validation results were consistent with the high-throughput sequencing findings.

Discussion

In this study, we identified the jointly differentially expressed miRNAs in the serum exosomes of advanced GC patients with distinct therapeutic responses to PD-1 monoclonal antibody therapy combined with chemotherapy, underscoring the utility of miRNAs as potential biomarkers

Table 2 Demographic and clinical characteristics of validation cohort patients (n=6)

Characteristics	Responder (n=3)	Non-responder (n=3)
Age, median [range]	63 [63–78]	67 [66–69]
Gender, n (%)		
Female	3 (100.00)	1 (33.33)
Male	0	2 (66.67)
PD-L1 (CPS), n (%)		
>10	0	0
1–10	2 (66.67)	1 (33.33)
<1	1 (33.33)	2 (66.67)
Tumor location, n (%)		
Fundus of stomach	0	1 (33.33)
Antrum	1 (33.33)	1 (33.33)
Lesser curvature of stomach	1 (33.33)	1 (33.33)
Greater curvature	1 (33.33)	0
MMR/MSI, n (%)		
MSS	3 (100.00)	3 (100.00)
Histology differentiation, n (%)		
Well	1 (33.33)	1 (33.33)
Moderately	0	2 (66.67)
Poorly	2 (66.67)	0

PD-L1, programmed death-ligand 1; CPS, combined positive score; MMR, mismatch repair; MSI, microsatellite instability; MSS, microsatellite stability.

for therapeutic efficacy prediction. Specifically, we found that the increased expression of miR-451a and miR-142-5p may serve as indicators for identifying patients likely to benefit from this treatment regimen.

Immunotherapy holds promise as an effective treatment for advanced GC; however, only a minority of patients derive significant benefits, while others experience limited or adverse responses. Current stratification methods based on tumor tissue PD-L1 expression lack accuracy, necessitating the exploration of more precise biomarkers. MiRNAs, small non-coding RNA molecules, play crucial roles in various cellular processes, including transcription, cell fate determination, and metabolism. Emerging evidence suggests their diagnostic, therapeutic, and predictive potential in diverse diseases, including digestive tract tumors. Notably, functional plasma exosomal miRNAs hold promise as biomarkers for GC, and their differential expression has been found to be correlated with therapeutic efficacy and prognosis (12,13). One study of the peripheral blood miRNA profiles of non-small cell lung cancer patients identified potential peripheral blood biomarkers for predicting immunotherapy response (14). Researchers introduced a five-miRNA risk-score model as a potential blood-based adjunctive diagnostic tool, which surpassed tissue-based PD-L1 staining in terms of diagnostic accuracy and predictive efficacy for patient response to therapy. A further enrichment analysis revealed significant interactions between PD-L1 pathway genes and miRNA target genes, indicating potential regulatory mechanisms. For example, MAPK signaling pathways were found to be highly enriched in multiple miRNA target genes, which is consistent with

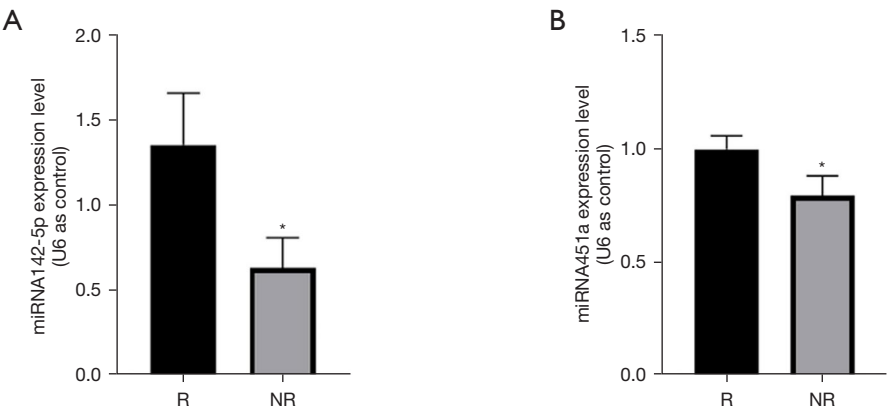

Figure 4 MiRNA451a and miRNA142-5p were upregulated in the responder group. qPCR analysis of miRNA451a (A) and miRNA142-5p (B) in the plasma of six patients after treatment with the camrelizumab and SOX regimen. The data were normalized with U6 values. *, P<0.05. R, responder group; NR, non-responder group; qPCR, quantitative polymerase chain reaction; SOX, S-1 plus oxaliplatin.

our findings for GC. This alignment suggests a potential functional link between the PD-L1/PD-1 pathway and upstream MAPK signaling.

MiRNAs also play a crucial role in regulating the immune microenvironment, thereby affecting the efficacy of PD-1 monoclonal antibody therapy. Specifically, in cancer patients, following the persistent exposure of T cells to antigens, specific cluster of differentiation 8$^+$ (CD8$^+$) T cells may undergo depletion, resulting in reduced anti-tumor activity (15). A study has shown that the activation of CD8$^+$ T cells stimulates the expression of miR-31 via T-cell receptor signaling, leading to the activation of downstream nuclear factors in T cells, which subsequently reduces the anti-tumor activity of these cells. However, the knockout of miR-31 in CD8$^+$ T cells resulted in the increased expression of genes related to T cell function and activation, which suggests that targeting miR-31 could enhance immunotherapy efficacy (16). Moreover, the identification of the different miRNAs associated with clinical efficacy not only aids in predicting the immunotherapy response, but could also lead to the development of combination therapy models. For example, one study observed an increase in miR-21-3p levels in tumors, which could enhance the efficacy of anti-PD-1 immunotherapy by regulating iron-mediated tumor cell death. The upregulation of miR-21-3p promotes interferon-γ-mediated iron death by enhancing lipid peroxidation. In preclinical mouse models, gold nanoparticles loaded with miR-21-3p improved the efficacy of anti-PD-1 antibodies, revealing the therapeutic potential of miRNA-based treatments (17). These findings emphasize the intricate interplay between miRNAs, immune checkpoint pathways, and tumor microenvironment dynamics in modulating the immunotherapy response, and highlight the potential of miRNA-based therapeutics and combination strategies in enhancing anti-tumor immune responses and improving the clinical outcomes of cancer patients.

In our study, we identified two significantly elevated miRNAs (i.e., miR-451a and miR-142-5p), which have been previously reported to be associated with GC. This observation aligns with previous research indicating that miR-451a influences GC cells through the PI3K-AKT-mTOR pathway. The downregulation of miR-451a in primary GC tissues and cell lines resulted in decreased cell viability, colony formation, migration, and invasion. Notably, the exogenous expression of miR-451a led to the reduced expression of its target genes, including mTOR, PI3K, and TSC1, indicating its potential tumor-inhibitory role in GC (18,19). Similarly, the upregulation of miR-142-5p was found to inhibit the development of GC by targeting lipoprotein receptor associated protein 8 (20). The reduced expression of miR-142 in GC tissues and cells was inversely correlated with lymph node metastasis and a poor prognosis in patients. The stable overexpression of miR-142 *in vitro* inhibited cell proliferation, migration, and invasion, underscoring its potential as a therapeutic target in GC (21,22). In this study, we found that levels of miR-451a and miR-142 were significantly elevated in patients who exhibited effective therapeutic responses to carrilizumab combined with chemotherapy for advanced GC. These findings suggest that these mRNAs could serve as prognostic biomarkers for predicting the clinical efficacy and outcomes of the PD-1 monoclonal immunotherapy treatment strategy in GC.

Further, GO and KEGG enrichment analyses were performed to investigate the potential regulatory functions and specific molecular mechanisms of these miRNA target genes. The KEGG pathway analysis revealed enrichment in signal transduction pathways, such as metabolic pathways, axonal guidance, and calcium signaling pathways (RAP1, RAS, and PI3K-AKT), indicating the multifaceted involvement of upregulated miRNAs in various BPs. Importantly, we uncovered the regulatory roles of various miRNAs in the PI3K-AKT-MTOR pathway, with the PTEN protein emerging as a central factor influencing this pathway. A recent clinical study has shown the significance of PTEN in the solid tumor invasion of T cells and immune checkpoint therapy response. The successful restoration of PTEN function significantly induced immunogenic cell death and reversed the tumor immunosuppressive microenvironment, ultimately enhancing anti-tumor immunotherapy efficacy (23). Thus, elucidating how different miRNAs modulate this pathway and its key proteins represents a critical focus for future research.

This study had some limitations. Notably, the inclusion of only a single hospital with a small patient cohort necessarily makes these findings hypothesis-generating only. While our results suggest that miR-451a and miR-142-5p hold potential as predictive biomarkers for immunochemotherapy response in gastric cancer, further studies with larger and more diverse patient cohorts are needed to validate these preliminary findings. Additionally, although bioinformatics analysis indicated that these miRNAs may regulate transcription factors and cell cycle-related proteins, their roles in intercellular signaling and immune response modulation require further *in vivo* and

in vitro investigation to better establish their mechanistic relevance in gastric cancer. Future research expanding upon these exploratory results will be essential to confirm the clinical utility of miR-451a and miR-142-5p. Importantly, the clinical implications of these findings warrant careful consideration. The identification of specific miRNAs as potential biomarkers for predicting PD-1 therapy efficacy highlights their role in advancing personalized therapy for gastric cancer. These miRNAs could serve as predictive tools in clinical settings, ultimately improving treatment decision-making and outcomes for GC patients.

Conclusions

In summary, our findings indicate that advanced GC patients who may respond to PD-1 monoclonal immunotherapy have distinct circulating exosome-derived RNA profiles compared to non-responders. Specifically, we identified and validated the predictive potential of miR-451a and miR-142-5p in GC. A miRNA-based liquid biopsy model with promising sensitivity and specificity for predicting responders should be developed. Our results suggest a potential application of these miRNAs in clinical practice to guide treatment strategies, paving the way for precision medicine in gastric cancer. Further exploration into these biomarkers may lead to robust, non-invasive methods for personalizing therapeutic approaches, ultimately improving the standard of care in GC.

Acknowledgments

We would like to thank the employees of Zhaoqing Zheng from Jiangsu Hengrui Pharmaceuticals Co., Ltd. for their assistance in writing this article. We would also like to thank Professor Shao Guo and his team at Longgang Third People's Hospital, Shenzhen for their support.

Funding: This study was funded by grants from the Baotou Health Science and Technology Program Project Subjects (No. wsjkkj2022002), the "Grassland Talent" Project Special Funding Support Program (No. CYYC230416), the Project of Inner Mongolia Natural Science Foundation of Inner Mongolia Autonomous Region (No. 2024MS08047), the National Natural Science Foundation of China (Nos. 81660307 and 82060337), the Shenzhen Longgang District Economic and Technological Development Special Fund Medical, Health Technology Plan Project (Nos. LGKCYLWS2021000033 and LGKCYLWS2023025), and the Shenzhen Science and Technology Plan Project (Nos. JCYJ20220531092412028 and JCYJ20230807121306012).

Footnote

Reporting Checklist: The authors have completed the MDAR reporting checklist. Available at https://tcr.amegroups.com/article/view/10.21037/tcr-24-2151/rc

Data Sharing Statement: Available at https://tcr.amegroups.com/article/view/10.21037/tcr-24-2151/dss

Peer Review File: Available at https://tcr.amegroups.com/article/view/10.21037/tcr-24-2151/prf

Conflicts of Interest: All authors have completed the ICMJE uniform disclosure form (available at https://tcr.amegroups.com/article/view/10.21037/tcr-24-2151/coif). G.K. receives grants from AstraZeneca, BMS, CARsgen, Daiichi Sankyo, I-MAB, Jazz, Merck, Oncolys, Pieris, Triumvira, Zymeworks, and consulting fees from Astellas, AstraZeneca, Bayer, BMS, Daiichi Sankyo, I-MAB, Jazz, Merck, Oncolys, Pieris, Zymeworks, and gets support for attending meetings from Dava Oncology, I-MAB, outside the submitted work. Q.L. is an employee of Lianchuan Biotechnology Co., Ltd. The other authors have no conflicts of interest to declare.

Ethical Statement: The authors are accountable for all aspects of the work in ensuring that questions related to the accuracy or integrity of any part of the work are appropriately investigated and resolved. The study was conducted in accordance with the Declaration of Helsinki (as revised in 2013). The study was approved by the Ethics Committee of the Baotou Cancer Hospital (No. 2023001) and informed consent was taken from all the patients.

References

1. Bray F, Laversanne M, Sung H, et al. Global cancer

statistics 2022: GLOBOCAN estimates of incidence and mortality worldwide for 36 cancers in 185 countries. CA Cancer J Clin 2024;74:229-63.
2. Xia C, Dong X, Li H, et al. Cancer statistics in China and United States, 2022: profiles, trends, and determinants. Chin Med J (Engl) 2022;135:584-90.
3. Xu J, Jiang H, Pan Y, et al. Sintilimab Plus Chemotherapy for Unresectable Gastric or Gastroesophageal Junction Cancer: The ORIENT-16 Randomized Clinical Trial. JAMA 2023;330:2064-74.
4. Rha SY, Oh DY, Yañez P, et al. Pembrolizumab plus chemotherapy versus placebo plus chemotherapy for HER2-negative advanced gastric cancer (KEYNOTE-859): a multicentre, randomised, double-blind, phase 3 trial. Lancet Oncol 2023;24:1181-95.
5. Shitara K, Rha SY, Wyrwicz LS, et al. Neoadjuvant and adjuvant pembrolizumab plus chemotherapy in locally advanced gastric or gastro-oesophageal cancer (KEYNOTE-585): an interim analysis of the multicentre, double-blind, randomised phase 3 study. Lancet Oncol 2024;25:212-24.
6. Abd-Allah GM, Ismail A, El-Mahdy HA, et al. miRNAs as potential game-changers in melanoma: A comprehensive review. Pathol Res Pract 2023;244:154424.
7. Hu ML, Xiong SW, Zhu SX, et al. MicroRNAs in gastric cancer: from bench to bedside. Neoplasma 2019;66:176-86.
8. Deng C, Huo M, Chu H, et al. Exosome circATP8A1 induces macrophage M2 polarization by regulating the miR-1-3p/STAT6 axis to promote gastric cancer progression. Mol Cancer 2024;23:49.
9. Palamarchuk A, Tsyba L, Tomasello L, et al. PDCD1 (PD-1) is a direct target of miR-15a-5p and miR-16-5p. Signal Transduct Target Ther 2022;7:12.
10. Li Z, Suo B, Long G, et al. Exosomal miRNA-16-5p Derived From M1 Macrophages Enhances T Cell-Dependent Immune Response by Regulating PD-L1 in Gastric Cancer. Front Cell Dev Biol 2020;8:572689.
11. Zhang S, Liu S, Yue C, et al. Identification of necroptosis-associated miRNA signature for predicting prognosis and immune landscape in stomach adenocarcinoma. Exp Cell Res 2024;436:113948.
12. Berindan-Neagoe I, Monroig Pdel C, Pasculli B, et al. MicroRNAome genome: a treasure for cancer diagnosis and therapy. CA Cancer J Clin 2014;64:311-36.
13. Chen Y, Feng H, Wu Y, et al. Evaluation of plasma exosomal microRNAs as circulating biomarkers for progression and metastasis of gastric cancer. Clin Transl Med 2020;10:e171.
14. Rajakumar T, Horos R, Jehn J, et al. A blood-based miRNA signature with prognostic value for overall survival in advanced stage non-small cell lung cancer treated with immunotherapy. NPJ Precis Oncol 2022;6:19.
15. Yang Z, Liu L, Zhu Z, et al. Tumor-Associated Monocytes Reprogram CD8(+) T Cells into Central Memory-Like Cells with Potent Antitumor Effects. Adv Sci (Weinh) 2024;11:e2304501.
16. Moffett HF, Cartwright ANR, Kim HJ, et al. The microRNA miR-31 inhibits CD8(+) T cell function in chronic viral infection. Nat Immunol 2017;18:791-9.
17. Guo W, Wu Z, Chen J, et al. Nanoparticle delivery of miR-21-3p sensitizes melanoma to anti-PD-1 immunotherapy by promoting ferroptosis. J Immunother Cancer 2022;10:e004381.
18. Riquelme I, Tapia O, Leal P, et al. miR-101-2, miR-125b-2 and miR-451a act as potential tumor suppressors in gastric cancer through regulation of the PI3K/AKT/mTOR pathway. Cell Oncol (Dordr) 2016;39:23-33.
19. Streleckiene G, Inciuraite R, Juzenas S, et al. miR-20b and miR-451a Are Involved in Gastric Carcinogenesis through the PI3K/AKT/mTOR Signaling Pathway: Data from Gastric Cancer Patients, Cell Lines and Ins-Gas Mouse Model. Int J Mol Sci 2020;21:877.
20. Lu J, Ma Y, Zhao Z. MiR-142 suppresses progression of gastric carcinoma via directly targeting LRP8. Clin Res Hepatol Gastroenterol 2021;45:101520.
21. Yan J, Yang B, Lin S, et al. Downregulation of miR-142-5p promotes tumor metastasis through directly regulating CYR61 expression in gastric cancer. Gastric Cancer 2019;22:302-13.
22. Zhang X, Yan Z, Zhang J, et al. Combination of hsa-miR-375 and hsa-miR-142-5p as a predictor for recurrence risk in gastric cancer patients following surgical resection. Ann Oncol 2011;22:2257-66.
23. Lin YX, Wang Y, Ding J, et al. Reactivation of the tumor suppressor PTEN by mRNA nanoparticles enhances antitumor immunity in preclinical models. Sci Transl Med 2021;13:eaba9772.

(English Language Editor: L. Huleatt)

Cite this article as: Hua Y, Luo S, Li Q, Song G, Tian X, Wang P, Zhu H, Lv S, Zhang X, Yang Z, Ku G, Shao G. The efficacy of plasma exosomal miRNAs as predictive biomarkers for PD-1 blockade plus chemotherapy in gastric cancer. Transl Cancer Res 2024;13(11):6336-6346. doi: 10.21037/tcr-24-2151

